

## BIOPHYSICS AND BIOCHEMISTRY

# Thermodynamic Parameters of Melting and Stabilization of G-Actin Structure in the Norm and Cardiomyopathy

A. P. Kitaeva, Z. D. Tedeeva, and N. V. Karsanov

Translated from *Byulleten' Eksperimental'noi Biologii i Meditsiny*, Vol. 128, No. 7, pp. 35-38, July, 1999  
Original article submitted August 17, 1998

Differential scanning microcalorimetry showed that calorimetric enthalpy of melting of purified G-actin from canine myocardium is decreased in L-thyroxin-induced cardiomyopathy. By contrast, in athyroid cardiomyopathy this parameter increases almost 2-fold mainly due to the increase in excess heat capacity in a low-temperature region of the thermogram caused by melting of the small domain in the monomer. The pathological process in both cases is accompanied by contractility disturbances.

**Key Words:** *G-actin; thermodynamics; athyroid cardiomyopathy; L-thyroxin cardiomyopathy*

It was previously established that 2-3-month-long cardiac insufficiency caused by L-thyroxin-induced (LTC) and athyroid (ATC) cardiomyopathy (or myocardial dystrophy according to G. F. Lang) strongly impairs polymerization of actin in human or animal myocardium [9]. According to circular dichroism data, the conformation of G- and F-actins changes drastically [3]; hybrid actomyosin containing actin from the *post mortem* myocardium of a patient dead from cardiac insufficiency [8] superprecipitates (contracts [7]) much more weaker than actomyosin containing normal actin.

Our aim was to study thermodynamic parameters of melting of G-actin from canine myocardium in LTC and ATC.

## MATERIALS AND METHODS

Experiments were carried out on 16 male mongrel dogs: control animals ( $n=5$ ) and dogs with LTC ( $n=6$ ) and ATC ( $n=5$ ). The dogs were maintained under vivarium conditions on a standard ration. The animals were euthanized under hexenal narcosis.

LTC was induced by daily treatment with L-thyroxin (0.7 mg/kg *per os* [11]), and ATC was modeled by thyroidectomy [1]. G-actin was isolated from acetone-dried powder of the septum and left and right ventricles [13].

Purity of the protein was controlled by electrophoresis in 11% SDS PAAG. Protein concentration was determined by the biuret method.

Actin molecular weight was taken to be 42 kD. Melting was studied on a DASM-4A differential adiabatic scanning microcalorimeter (Pushchino) with computer monitoring and automatic data processing. The volume of the calorimetric cell was 1 ml and scanning rate was 2 K/min. Change in calorimetric enthalpy ( $\Delta H^{CAL}$ ) during melting of G-actin was determined by the intensity of heat absorption:  $\Delta H^{CAL} = \Delta Q/m$ , where  $\Delta Q$  is the heat corresponding to the area under the thermogram of excess heat capacity, and  $m$  is protein content in the cell (in moles). Vant Hoff effective enthalpy ( $\Delta H^{VH}$ ) was calculated by the formula [5]:

$$\Delta H^{VH} = 2T^M \sqrt{R\Delta C_p^M},$$

where  $T^M$  is temperature (in K) in the melting peak,  $\Delta C_p^M$  is maximum partial heat capacity of protein tran-

sition from the native to denaturated states, and  $R$  is the Boltzmann constant  $8.31 \text{ J}/(\text{mol}\times\text{K})$ .

Irreversible course of G-actin denaturation was controlled after its cooling by repeated heating in the calorimetric cell.

The melting cooperativity index  $N=\Delta H^{\text{VH}}/\Delta H^{\text{CAL}}$  was used to evaluate the intermediate states of the protein during thermal denaturation.  $N>1$  was interpreted as enhanced interdomain interaction or aggregation of the protein micellae, while  $N\leq 1$  indicates multiplicity of transition in the molecule [2,4-6,14].

All measurements were carried out in a medium containing (in mM): 2 Tris HCl (pH 8.0), 0.2 Na-ATP, 0.2  $\text{CaCl}_2$ , 1  $\text{NaN}_3$ , and 0.5 dithiothreitol. The working protein concentrations were 1.2-1.5 mg/ml.

The standard thermodynamic parameters enthalpy ( $\Delta H^0$ ), entropy ( $\Delta S^0$ ), and free energy ( $\Delta G^0$ ) of stabilization of G-actin structure were calculated at  $25^\circ\text{C}$  as described previously [10,12].

The data were analyzed statistically as small independent groups.

## RESULTS

By visual estimation, the melting thermogram of myocardial G-actin from dogs with LTC did not significantly differ from the normal curve both at low and high ( $>45^\circ\text{C}$ ) temperatures (Fig. 1). However, there was a minor shift of the melting peak to a high temperature region.

In ATC, the melting thermogram of G-actin drastically differed from that observed in LTC and from normal curves: a pronounced flat peak of excess heat capacity appeared at low temperatures ( $20\text{-}30^\circ\text{C}$ ), which

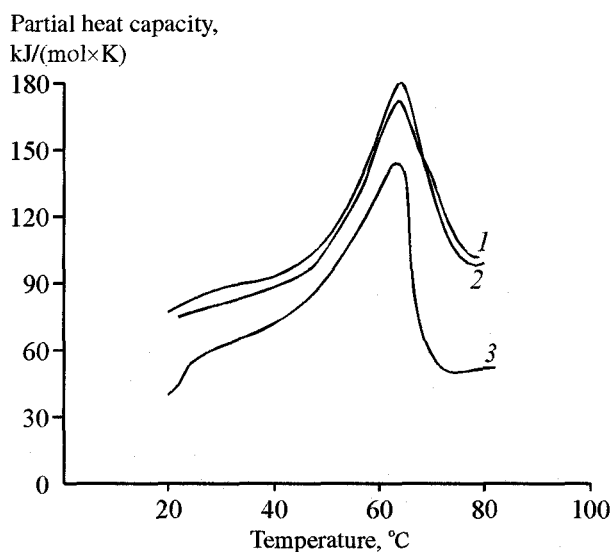


**Fig. 1.** Melting thermograms of purified myocardial G-actin from control dog (1) and animals with 2-3-month L-thyroxin-induced (2) or athyroid (3) cardiomyopathy.

**TABLE 1.** Thermodynamic Parameters of Melting and Stabilization of G-Actin from Canine Myocardium ( $M\pm m$ )

Group	$T^{\text{M}}, ^\circ\text{C}$	$\Delta H^{\text{CAL}}, \text{kJ/mol}$	$\Delta H^{\text{VH}}, \text{kJ/mol}$	$N$ , arb. units	$\Delta C_{\text{p}}^{\text{M}}, \text{kJ}/(\text{mol}\times\text{K})$	$\Delta S^{\text{M}}, \text{kJ}/(\text{mol}\times\text{K})$	$\Delta C_{\text{p}}^{\text{D}}, \text{kJ}/(\text{mol}\times\text{K})$	$\Delta H^0, \text{kJ/mol}$	$\Delta S^0, \text{kJ}/(\text{mol}\times\text{K})$	$\Delta G^0, \text{kJ/mol}$
Normal	$63.6\pm 0.3$	$619\pm 16$	$513\pm 20$	$0.80\pm 0.04$	$70.6\pm 5.6$	$1.83\pm 0.04$	$10.4\pm 0.2$	$212\pm 4$	$0.57\pm 0.01$	$44.6\pm 2.0$
LTC	$64.2\pm 0.2$	$507\pm 26^{**}$	$472\pm 19$	$0.91\pm 0.04$	$59.1\pm 5.0$	$1.50\pm 0.07^{**}$	$8.3\pm 0.4^{**}$	$181\pm 14$	$0.48\pm 0.04$	$38.1\pm 2.0^{***}$
ATC	$63.0\pm 0.4$	$1179\pm 26^{***}$	$613\pm 21^{**}$	$0.52\pm 0.02^{**}$	$100.8\pm 7.2^{**}$	$3.51\pm 0.07^{***}$	$7.8\pm 0.9^{**}$	$851\pm 72^{***}$	$2.69\pm 0.09^{***}$	$109.6\pm 4.0^{***}$

**Note.**  $\Delta S^{\text{M}}$  is entropy change during denaturation, and  $\Delta C_{\text{p}}^{\text{D}}$  is change of basic heat capacity after denaturation.  $^{*}p<0.05$ ,  $^{**}p<0.01$ ,  $^{***}p<0.001$  compared with the control.

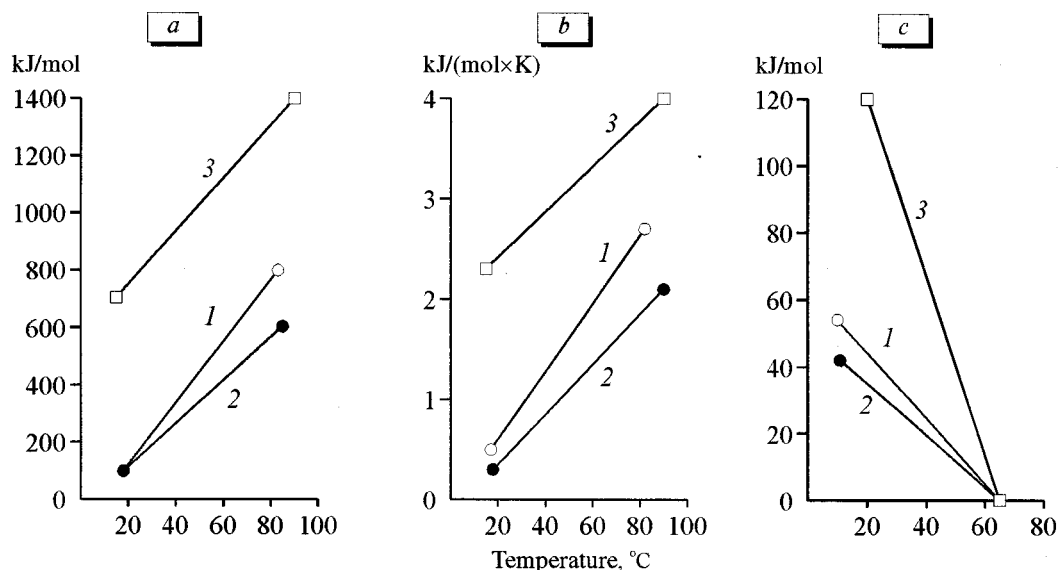


Fig. 2. Denaturation increment of changes in enthalpy (a), entropy (b), and free energy (c) of melting of myocardial G-actin from control dog (1) and animals with L-thyroxin-induced (2) or athyroid (3) cardiomyopathy.

attests to multiplicity of melting of the thermoliable fragment of G-actin and changes in the conformation stabilization energy of the small domain.

Both normal and LTC-modified actin are characterized by low excess heat capacity in the corresponding temperature regions.

$\Delta H^{\text{CAL}}$  of G-actin melting (including low- and high-temperature regions) significantly increased (2-fold) in ATC. As a result, the index of cooperativity drastically decreased (by 1.54 times). This indicates an increase in the multiplicity of melting and pronounced disturbances in G-actin structure. At the same time, an increase in the enthalpy of stabilization of G-actin structure was accompanied by a 5-fold increase in the entropy and 2.5-fold increase in free energy, which attests to profound conformational rearrangements induced by ATC (Table 1, Fig. 2).

In contrast,  $\Delta H^{\text{VH}}$  and, to a greater extent,  $\Delta H^{\text{CAL}}$  decreased in LTC. Correspondingly, the cooperativity index tended to 1, which attests to a decrease in multiplicity of melting.

All other thermodynamic parameters of melting also decreased in LTC (Table 1, Fig. 2). This tendency would be significant ( $p < 0.05$ ) after increasing the number of experiments from 6 to 8.

Analysis of the standard thermodynamic parameters showed that structure of G-actin in LTC is more stable than in normal myocardium. Maximum structural stability of G-actin ( $\Delta S = 0$ ,  $\Delta H > 0$ ,  $\Delta G = \text{max}$ ) in LTC can be achieved at a higher temperature than that of normal actin (4°C). In ATC,  $\Delta G$  attains a maximum at negative temperatures (Fig. 2), which attests to possible protein denaturation even at room temperature [10,12,14].

The increase in  $\Delta H^{\text{CAL}}$  and  $\Delta H^{\text{VH}}$  in ATC can be interpreted as condensation G-actin molecule in comparison with normal. However, this inference contradicts with the decrease in cooperativity index (Table 1). This combination of thermodynamic parameters rather corresponds to a structure with weakened inter-domain bonds and additional intradomain bonds resulting in local heterogeneities in the structure density. Judging from the low-temperature part of the thermogram [6], these changes are related predominantly to the small domain: translocation of hydrophobic groups from the surface to the core of the protein. In intact actin these groups are located in the cleft between domains and interact with the hydrophobic groups of the large domain. The ATC-induced redistribution of chemical bonds (caused by weakening of the inter-domain bonds) should widen the cleft and change the conformation of both domains, and to a greater extent the small domain. Moreover, widening of the cleft contributes to additional attachment of ions (in particular,  $\text{Ca}^{2+}$ ), because new charged regions can be exposed in the widened cleft. In this case, the excess heat capacity in ATC can be explained by the release of bound  $\text{Ca}^{2+}$  ions. Complete removal of  $\text{Ca}^{2+}$  from the medium (EGTA) eliminates all peaks of excess heat capacity caused by  $\alpha$ - $\beta$  transition during actin melting [6].

Therefore, the excess heat capacity of G-actin melting in ATC can originate from consolidation of hydrophobic package of actin domains (predominantly of the small domain) and the release of  $\text{Ca}^{2+}$  from additional binding sites.

Thus, both the increase and decrease in thyroxin transmitter function modifies the structure of G-actin: protein stability increased in LTC and decreased in

ATC, while functional activity of the contractile protein system is impaired in both cases. These findings suggest that conformation of intact G-actin is optimal for interaction with myosin, generation of the contraction force, and energy conversion. Deviation of this conformation from the optimum impairs functional characteristics of actin filaments.

## REFERENCES

1. Ya. M. Kabak, *Laboratory Course in Endocrinology* [in Russian], Moscow (1968).
  2. C. R. Cantor and P. R. Schimmel, *Biophysical Chemistry*, San Francisco (1980).
  3. N. V. Karsanov and B. G. Dzinchvelashvili, *Izv. Akad. Nauk Gruz. SSR, Ser. Biol.*, **14**, 134-142 (1988).
  4. P. L. Privalov, *Advances in Sciences and Technology, Ser. Mol. Biol.* [in Russian], Vol. 6, Moscow (1975), pp. 7-33.
  5. L. V. Tatunashvili and P. L. Privalov, *Biofizika*, **29**, 583-585 (1984).
  6. A. Bertazzon, G. H. Tian, A. Lamblin, and T. Tsong, *Biochemistry*, **29**, 291-298 (1990).
  7. S. Higashi-Fujimi, *J. Cell. Biol.*, **101**, 2335-2344 (1985).
  8. N. V. Karsanov, G. I. Nizharadze, M. P. Pirtskhalaishvili, *et al.*, *Gen. Physiol. Biophys.*, **4**, 417-423 (1985).
  9. N. V. Karsanov, M. P. Pirtskhalaishvili, V. I. Semerikova, and N. Sh. Losaberidze, *Basic Res. Cardiol.*, **81**, 199-212 (1986).
  10. S. Lapanje and N. Poklar, *Biophys. Chem.*, **34**, 155-162 (1989).
  11. D. A. Piatnac and R. E. Olson, *Fed. Proc.*, **15**, 145 (1956).
  12. P. L. Privalov and N. N. Khechinashvili, *J. Mol. Biol.*, **86**, 665-684 (1974).
  13. J. A. Spudich and S. Watt, *J. Biol. Chem.*, **246**, 4866-4871 (1971).
  14. T. N. Tsalcova and P. L. Privalov, *J. Mol. Biol.*, **181**, 533-544 (1985).
-